

## Kinetic model of the generalized Enskog equation for binary mixtures

L. Letamendia and G. Nouchi

*Centre de Physique Moléculaire Optique et Hertzienne, Université de Bordeaux I, 351 Cours de la Libération,  
F-33405 Talence, France*

Sidney Yip

*Department of Nuclear Engineering, Massachusetts Institute of Technology, Cambridge, Massachusetts 02139*

(Received 11 March 1985)

A kinetic model has been formulated based on the generalized Enskog equations for a binary mixture of hard-sphere fluids. The resulting description is an improvement over an existing model based on the linearized Boltzmann equations for Maxwell molecules in that effects of thermal diffusion and nonideality corrections are taken into account. It is shown that the present model gives results for density fluctuations in quantitative agreement with light-scattering spectra of Xe-He mixtures.

### I. INTRODUCTION

Kinetic model equations provide a tractable means of analysis, at the level of transport theory, of nonhydrodynamic behavior in fluids. One such application is the interpretation of light-scattering spectra of density fluctuations at wavelengths comparable to the collision mean-free path. As can be expected, kinetic models were first developed for pure fluids<sup>1</sup> before extensions were made to multicomponent mixtures.<sup>2</sup> For low-density fluids satisfactory kinetic models for both single-component fluids and binary mixtures have been derived from linearized Boltzmann equations. At higher densities where the thermodynamic properties of the fluid can no longer be described as those of an ideal gas, a kinetic model based on the generalized Enskog equation has been developed.<sup>3,4</sup> An attempt to derive a corresponding description for a binary mixture was also made.<sup>5</sup> However, the results of this formulation are not quite complete. Moreover, only limited numerical results were produced, and to perform further computations would require reprogramming the entire calculation.

In this paper we present a kinetic model description of density fluctuations in moderately dense binary mixtures. This work was motivated by the availability of Rayleigh-Brillouin spectra<sup>6</sup> of Xe-He mixtures which could not be explained satisfactorily by an existing kinetic model<sup>2</sup> for

low-density mixture of Maxwell molecules (atoms interacting through  $1/r^4$  potential). It has been pointed out<sup>7</sup> that the discrepancy is most likely due to the effects of thermal diffusion and nonideality, or imperfect-gas corrections, both not taken into account in the existing kinetic model. We will show that the present formulation gives numerical results that are in quantitative agreement with the experimental spectra and go over correctly to the pure-fluid limit. On this basis one can conclude that a successful development of a kinetic model for moderately dense binary-fluid mixtures, in particular, one which treats thermal diffusion and nonideality corrections, has been achieved.

In Sec. II we introduce the generalized Enskog kinetic equations for a hard-sphere mixture with explicit contributions to the memory function or collision operator from static interactions and collisions. A kinetic model is then derived by using a matrix representation of the memory function, retaining in full the low-order matrix elements, and approximating the remainder by a diagonal matrix with all elements equal to a constant. In Sec. III the various matrix elements used in formulating the kinetic model are given explicitly, and in Sec. IV details of numerical calculations are given along with a demonstration that the model reduces properly to the case of a pure fluid. The analysis of light-scattering spectra in Xe-He mixtures is carried out in Sec. V, and we conclude with a few remarks in Sec. VI.

### II. KINETIC MODEL FORMULATION

#### A. General equations

We define the phase-spacing density correlation function, following the notations of Ref. 5,

$$C_{\alpha\beta}(\mathbf{r}-\mathbf{r}', \mathbf{p}, \mathbf{p}', t-t') = \langle [f^\alpha(\mathbf{r}, \mathbf{p}, t) - \langle f^\alpha(\mathbf{r}, \mathbf{p}, t) \rangle] [f^\beta(\mathbf{r}', \mathbf{p}', t') - \langle f^\beta(\mathbf{r}', \mathbf{p}', t') \rangle] \rangle, \quad (2.1)$$

where

$$f^\alpha(\mathbf{r}, \mathbf{p}, t) = \sum_{j=1}^{N_\alpha} \delta(\mathbf{r} - \mathbf{R}_j^\alpha(t)) \delta(\mathbf{p} - \mathbf{P}_j^\alpha(t)). \quad (2.2)$$

For a binary mixture of atom species  $a$  and  $b$ , indices  $\alpha$  and  $\beta$  can be either  $a$  or  $b$ . The Fourier-Laplace transform of (2.1) will be denoted as

$$S^{\alpha\beta}(\mathbf{k}, \mathbf{p}, \mathbf{p}', z) = -i \int d^3r \int_0^\infty dt e^{-i(\mathbf{k}\cdot\mathbf{r} - zt)} C_{\alpha\beta}(\mathbf{r}, \mathbf{p}, \mathbf{p}', t). \quad (2.3)$$

This correlation function satisfies the kinetic equation

$$\left[ z - \frac{\mathbf{k}\cdot\mathbf{p}}{m_\alpha} \right] S^{\alpha\beta}(\mathbf{k}, \mathbf{p}, \mathbf{p}', z) - \int d^3p'' \phi_{\alpha\gamma}(\mathbf{k}, \mathbf{p}, \mathbf{p}'', z) S^{\gamma\beta}(\mathbf{k}, \mathbf{p}'', \mathbf{p}', z) = -\tilde{S}^{\alpha\beta}(\mathbf{k}, \mathbf{p}, \mathbf{p}') \quad (2.4)$$

characterized by the frequency and wave-number-dependent phase-space memory function  $\phi_{\alpha\beta}$ .

There are three contributions to the memory function,<sup>5</sup>

$$\phi_{\alpha\beta}(\mathbf{k}, \mathbf{p}, \mathbf{p}', z) = \phi_{\alpha\beta}^s(\mathbf{k}, \mathbf{p}) + \delta_{\alpha\beta} \phi_{\alpha\beta}^{\text{dc}}(\mathbf{k}, \mathbf{p}, \mathbf{p}', z) + \phi_{\alpha\beta}^{\text{cc}}(\mathbf{k}, \mathbf{p}, \mathbf{p}', z). \quad (2.5)$$

The static part of the memory function  $\phi^s$  which represents the effects of restoring forces due to spatial correlations with neighboring atoms has the form

$$\phi_{\alpha\beta}^s(\mathbf{k}, \mathbf{p}) = -(n_\alpha \mathbf{k}\cdot\mathbf{p}/m_\alpha) \Phi_\alpha(p) C_{\alpha\beta}^D(k) \quad (2.6)$$

where  $n_\alpha$  and  $m_\alpha$  are the number density and mass of atom  $\alpha$ ,  $\Phi_\alpha(p)$  is the Maxwellian distribution,

$$\Phi_\alpha(p) = \left[ \frac{\beta}{2\pi m_\alpha} \right]^{3/2} e^{-\beta p^2/2m_\alpha} \quad (2.7)$$

with  $\beta^{-1} = k_B T$ , and  $C_{\alpha\beta}^D(k)$  is the direct correlation function for the mixture system. For low density its value is

$$C_{\alpha\beta}^D(k) = -\frac{4\pi}{k} \sigma_{\alpha\beta}^2 j_1(k\sigma_{\alpha\beta}), \quad (2.8)$$

where  $\sigma_{\alpha\beta} = (\sigma_\alpha + \sigma_\beta)/2$ ,  $\sigma_\alpha$  is the hard-sphere diameter of atom  $\alpha$ , and  $j_1$  is the first-order spherical Bessel function.

The direct collision term  $\phi_{\alpha\beta}^{\text{dc}}$  can be expressed as a special case of the cross collision contribution and is equivalent to the memory function for a one-component fluid.<sup>7</sup> For a moderate-density binary mixture one has<sup>5</sup>

$$\begin{aligned} \phi_{\alpha\beta}^{\text{cc}}(\mathbf{k}, \mathbf{p}, \mathbf{p}') \Phi_\beta(p') &= i n_\beta \sigma_{\alpha\beta}^2 g_{\alpha\beta}(\sigma_{\alpha\beta}) \left[ \frac{\beta}{\pi(m_\alpha m_\beta)^{1/2}} \right]^3 \\ &\times \int d^3P d^3P_r d\Omega_r \exp \left[ -\beta \left( \frac{P_r^2}{2m_r} + \frac{2P^2}{M} \right) \right] \Theta(-\hat{\mathbf{r}}\cdot\mathbf{p}_r) \exp[i\mathbf{k}\cdot\hat{\mathbf{r}}\sigma_{\alpha\beta}(1-\delta_{\alpha\beta})] \delta(\mathbf{p}' - (2m_\beta/M)\mathbf{P} - \mathbf{p}_r) \\ &\times [\delta(\mathbf{p} - (2m_\alpha/M)\mathbf{P} + (1-2\delta_{\alpha\beta})\mathbf{p}_r) - \delta(\mathbf{p} - (2m_\alpha/M)\mathbf{P} + (1-2\delta_{\alpha\beta})\mathbf{P}_r^*)] \\ &- n_\alpha (1-\delta_{\alpha\beta}) \frac{\mathbf{k}\cdot\mathbf{p}}{m_\alpha} g_{\alpha\beta}(\sigma_{\alpha\beta}) \frac{4\pi\sigma_{\alpha\beta}^2}{k} j_1(k\sigma_{\alpha\beta}) \Phi_\alpha(p) \Phi_\beta(p'), \end{aligned} \quad (2.9)$$

where  $M = m_a + m_b$ ,  $m_r = m_a m_b / M$ ,  $\Theta$  the unit step function, the asterisk (\*) denotes post-collision momentum, and index  $\bar{\alpha}$  denotes the species other than  $\alpha$ . In (2.9)  $g_{\alpha\beta}(\sigma_{\alpha\beta})$  is the pair distribution function at contact. To obtain  $\phi_{\alpha\beta}^{\text{dc}}$ , we use the relation,

$$\phi_{\alpha\alpha}^{\text{dc}} = \phi_{\alpha\alpha}^{\text{cc}} + (\phi_{\alpha\bar{\alpha}}^{\text{cc}})_{\bar{\alpha}=\alpha}. \quad (2.10)$$

Equation (2.4) with the memory function given by Eq. (2.5), has been called the generalized Enskog equation.<sup>5</sup>

The initial value  $\tilde{S}_\alpha(\mathbf{k}, \mathbf{p}, \mathbf{p}')$  of the density correlation function has the form

$$\begin{aligned} \tilde{S}_\alpha(\mathbf{k}, \mathbf{p}, \mathbf{p}') &= n_\alpha \Phi_\alpha(p) \delta(\mathbf{p} - \mathbf{p}') \\ &+ n_\alpha n_\beta \Phi_\alpha(p) \Phi_\beta(p') h_{\alpha\beta}(k), \end{aligned} \quad (2.11)$$

where  $h_{\alpha\beta}(k)$  is the Fourier transform of  $g_{\alpha\beta}(r) - 1$ .

## B. Kinetic model

To extract the density correlation function measured by light-scattering experiment from Eq. (2.4) we will approximate the memory function by using a kinetic model.<sup>8</sup>

We will follow the procedure of Ref. 5 by choosing a basis function for the expansion

$$\psi_{lmn}(\xi) = |l m n\rangle = (l! m! n!)^{-1/2} \bar{H}_l(\xi_x) \bar{H}_m(\xi_y) \bar{H}_n(\xi_z), \quad (2.12)$$

where  $\bar{H}_l(x) = 2^{-l/2} H_l(x/\sqrt{2})$ ,  $H_l$  being the Hermite polynomial, and  $\xi = \mathbf{p}/m v_0$  is the reduced linear momentum with  $v_0^2 = (m\beta)^{-1}$ . Since this basis is complete and orthonormal, the memory function can be written as

$$\phi^{\alpha\beta}(\mathbf{k}, \xi, \xi') = \sum_{ij} \psi_i(\xi) \psi_j(\xi') \Phi(\xi) M_{\alpha\beta}(i|j), \quad (2.13)$$

where  $i \equiv (l, m, n)$ ,  $j \equiv (l', m', n')$ , and the matrix elements

of the memory function are defined by

$$M_{\alpha\beta}(i,j) = \int d^3\xi d^3\xi' \psi_i(\xi)\psi_j(\xi')\phi_{\alpha\beta}(\mathbf{k},\xi,\xi')\Phi(\xi) \\ = \langle lmn | \phi_{\alpha\beta} | l'm'n' \rangle. \quad (2.14)$$

The basic idea of the kinetic model is to treat the hydrodynamic states correctly by including in  $M_{\alpha\beta}$  the low-order matrix elements. For most of the nonhydrodynamic states one assumes that the off-diagonal elements in  $M_{\alpha\beta}$  can be neglected and that the diagonal elements can be replaced by a constant. Formally one writes

$$M_{\alpha\beta}(i | j) = -i v_{\alpha\beta}^N \delta_{ij}, \quad i, j > N \quad (2.15)$$

and  $v_{\alpha\beta}^N$  is the closure element.

Applying the expansion (2.12) to (2.4) and defining

$$h_{ij}^{\alpha\beta}(\mathbf{k},z) = \frac{1}{n_\alpha} \int d^3\xi d^3\xi' S^{\alpha\beta}(\mathbf{k},\xi,\xi',z)\psi_i(\xi)\psi_j(\xi') \quad (2.16)$$

we obtain a system of coupled matrix equations

$$(\underline{I} - i\underline{E}^a)\underline{h}^{aa} - i\underline{F}^b\underline{h}^{ba} = \underline{R}_1, \\ (\underline{I} - i\underline{E}^b)\underline{h}^{ba} - i\underline{F}^a\underline{h}^{aa} = \underline{R}_2, \quad (2.17)$$

where  $\underline{I}$  is unit matrix and the various parameters and matrices are defined below:

$$\underline{E}^a = \underline{D}^b(Y_a \gamma^{aa} \mathbf{1} + Y_{ab} \Gamma^{aa}) - i Y_{ab} Y_{ba} L^{ab} L^{ba} \underline{C} \Gamma^{ba}, \\ \underline{F}^b = \underline{D}^b Y_{ab} L^{ab} \Gamma^{ab} - i \underline{C} L^{ab} (Y_b Y_{ab} \gamma^{bb} + Y_{ab} Y_{ba} \Gamma^{bb}), \\ \underline{R}_1 = z_b \underline{C}^{DA} - i Y_{ab} \left[ \frac{\gamma}{v} \right]^{1/2} L^{ab} \underline{C}^{BA} - \underline{D}^{DA}, \\ \underline{R}_2 = z_a \left[ \frac{\gamma}{v} \right]^{1/2} \underline{C}^{BA} - i Y_{ba} L^{ba} \underline{C}^{DA} - \underline{D}^{BA} \left[ \frac{\gamma}{v} \right]^{1/2}, \quad (2.18)$$

where

$$v = 2m_a/M, \quad \gamma = 2m_b/M, \quad D^\alpha = Z_\alpha \underline{C} - \underline{D}, \\ Y_\alpha = \frac{n_\alpha \alpha_{\alpha\alpha}^N}{\sqrt{2} k v_0^\alpha}, \quad Y_{\alpha\beta} = \frac{n_\beta \Lambda_{\alpha\alpha}^N}{\sqrt{2} k v_0^\alpha}, \quad L^{\alpha\beta} = \Lambda_{\alpha\beta}^N / \Lambda_{\alpha\alpha}^N. \quad (2.19)$$

Here  $\alpha_{\alpha\alpha}^N$  and  $\Lambda_{\alpha\beta}^N$  are closure matrix elements expressions which are given in the next section. In (2.18)  $z_\alpha = X_\alpha + i(Y_\alpha + Y_{\alpha\beta})$ , where  $X_\alpha$  is the reduced frequency,  $X = \omega / \sqrt{2} k v_0^\alpha$  with  $(v_0^\alpha)^2 = k_B T / m_\alpha$ . In (2.19)  $\underline{C}$  and  $\underline{D}$  are matrices connected to plasma dispersion function<sup>9</sup>

$$C_{ij} = \frac{1}{\pi^{3/2}} \int \frac{\psi_i(\sqrt{2}\xi)\psi_j(\sqrt{2}\xi)e^{-\xi^2}}{(\xi_3 - z_a)(\xi_3 - z_b) + Y_{ab} Y_{ba} L^{ab} L^{ba}} d^3\xi, \\ D_{ij} = \frac{1}{\pi^{3/2}} \int \frac{\xi_3 \psi_i(\sqrt{2}\xi)\psi_j(\sqrt{2}\xi)e^{-\xi^2}}{(\xi_3 - z_a)(\xi_3 - z_b) + Y_{ab} Y_{ba} L^{ab} L^{ba}} d^3\xi, \quad (2.20)$$

where  $\xi_3$  is along an axis in the  $\mathbf{k}$  direction. Also in (2.18)  $\gamma^{\alpha\alpha}$  and  $\Gamma^{\alpha\beta}$  are matrices which contain memory-function matrix elements

$$\gamma_{ij}^{\alpha\alpha} = \delta_{ij} - i \frac{L_{ij}^{\alpha\alpha}}{\alpha_{\alpha\alpha}^N}, \quad (2.21)$$

$$\Gamma_{ij}^{\alpha\beta} = \delta_{ij} - i \frac{M_{ij}^{\alpha\beta}}{\Lambda_{\alpha\beta}^N}.$$

The elements  $L_{ij}^{\alpha\alpha}$  and  $M_{ij}^{\alpha\beta}$  are given in Sec. III. In (2.18)  $\underline{R}_1$  and  $\underline{R}_2$  are given by the matrices

$$(\underline{C}^{DA})_{ij} = C_{ij} \quad \text{if } j \neq 1, \\ (\underline{C}^{DA})_{i1} = C_{i1} S^{AA}(k), \\ (\underline{C}^{BA})_{ij} = C_{ij} \quad \text{if } j \neq 1, \\ (\underline{C}^{BA})_{i1} = C_{i1} S^{BA}(k), \\ (\underline{D}^{DA})_{ij} = D_{ij} \quad \text{if } j \neq 1, \\ (\underline{D}^{DA})_{i1} = D_{i1} S^{AA}(k), \\ (\underline{D}^{BA})_{ij} = D_{ij} \quad \text{if } j \neq 1, \\ (\underline{D}^{BA})_{i1} = D_{i1} S^{BA}(k), \quad (2.22)$$

where  $S_{\alpha\beta} = \delta_{\alpha\beta} - 4\pi[j_1(X_{\alpha\beta})/X_{\alpha\beta}]\rho_{\alpha\beta}$ , and  $\rho_{\alpha\beta} = n_\alpha \sigma_{\alpha\beta}^3$  is the density,  $X_{\alpha\beta} = k \sigma_{\alpha\beta}$  and  $j_1$  is the first-order spherical Bessel function.

From the solutions of Eqs. (2.17) we can calculate the dynamical structure factors  $S_{\alpha\beta}(\mathbf{k},\omega)$  defined by

$$S_{\alpha\beta}(\mathbf{k},\omega) = 2 \text{Im} \left[ \int d^3p d^3p' S_{\alpha\beta}(\mathbf{k},\mathbf{p},\mathbf{p}',z) \right]_{z=\omega+i0^+}. \quad (2.23)$$

These are the quantities needed to analyze the light-scattering spectra.

### III. MATRIX ELEMENTS OF MEMORY FUNCTION

The matrix elements of the memory function which we will take into account explicitly are those associated with the states  $|000\rangle$ ,  $|001\rangle$ , and

$$|E\rangle = \frac{1}{\sqrt{3}}(|002\rangle + |020\rangle + |200\rangle), \\ |\sigma\rangle = \left[ \frac{3}{2} \right]^{1/2} \left[ |002\rangle - \frac{|E\rangle}{\sqrt{3}} \right], \\ |H\rangle = \frac{1}{\sqrt{5}}(|201\rangle + |021\rangle + \sqrt{3}|003\rangle), \quad (3.1)$$

which correspond to number density, linear momentum, energy, longitudinal stress tensor, and energy, respectively. The state used to evaluate the closure element is

$$|M\rangle = \frac{1}{\sqrt{15}}[\sqrt{3}(|400\rangle + |040\rangle + |004\rangle) \\ + \sqrt{2}(|220\rangle + |022\rangle + |202\rangle)]. \quad (3.2)$$

Transverse-momentum components,  $|010\rangle$  and  $|100\rangle$ , and transverse-stress tensor  $|011\rangle$  need not be considered here because they are uncoupled to the variables defining the dynamical structure factor  $S(\mathbf{k},\omega)$ .

We have evaluated the matrix elements of the memory functions given in (2.6), (2.9), and (2.10), using (2.14) and the states enumerated above. An illustration of such a calculation is given in the Appendix.

TABLE I.  $M_{ab}^{cc}(i|j)$  in units of  $n_a v_0^2 \sigma_{ab}^2 g_{ab} \sqrt{\pi\gamma}$ .

	$ 000\rangle$	$ 001\rangle$	$ E\rangle$	$ \sigma\rangle$	$ H\rangle$
$ 000\rangle$	0	0	0	0	0
$ 001\rangle$	0	$-i8j_0''$	$4\left[\frac{\pi v}{6\gamma}\right]^{1/2} j_1$	$\frac{8}{5}\left[\frac{\pi v}{3\gamma}\right]^{1/2} (j_1 - \frac{3}{2}j_3)$	$-i\frac{4\gamma j_0''}{\sqrt{10}}$
$ E\rangle$	0	$4\left[\frac{\pi}{6}\right]^{1/2} j_1$	$i\frac{8}{3}\sqrt{\gamma v} j_0$	$-i\frac{8\sqrt{2}}{3}\sqrt{\gamma v} j_2$	$6\left[\frac{\pi}{15}\right]^{1/2} v j_1$
$ \sigma\rangle$	0	$\frac{8\sqrt{\pi}}{15}\left[j_1 - \frac{3}{2}j_3\right]$	$-i\frac{8}{3}\sqrt{2}\sqrt{\gamma v} j_2$	$i\frac{16}{5}\sqrt{\gamma v}\left[\frac{6}{7}j_4 - \frac{10}{21}j_2 + \frac{j_0}{3}\right]$	$\frac{24}{5}v\left[\frac{\pi}{30}\right]^{1/2} (j_1 - \frac{3}{2}j_3)$
$ H\rangle$	0	$-i\frac{4\gamma j_0''}{\sqrt{10}}$	$6\left[\frac{\pi\gamma v}{15}\right]^{1/2} j_1$	$\frac{24}{5}\left[\frac{\pi\gamma v}{30}\right]^{1/2} (j_1 - \frac{3}{2}j_3)$	$-i\frac{27}{5}\gamma v j_0''$

### A. Matrix elements of $\phi^{cc}$ and $\phi^{dc}$

The results for matrix elements  $M_{aa}^{cc}(i|j)$  and  $M_{ab}^{cc}(i|j)$  are given in Tables I and II. The direct collision terms  $L^{aa}(i,j)$  are obtained by setting  $a=b$  and  $\gamma=v=1$  in the sum  $M_{aa}^{cc}(i|j) + M_{ab}^{cc}(i|j)$ .<sup>3</sup> These matrix elements are the same as those for the pure fluid plus an extra term coming from the state  $|\sigma\rangle$ .<sup>4</sup> For the cross collisions the closure elements are

$$\langle M | \phi_{aa}^{cc} | M \rangle = -2i n_b V_0^2 \sigma_{ab}^2 g_{ab} (\sigma_{ab}) \times (\pi\gamma)^{1/2} (\gamma^2 v - \frac{8}{5}\gamma v + \frac{8}{3}v), \quad (3.3)$$

$$\langle M | \phi_{ab}^{cc} | M \rangle = 2i n_a V_0^2 \sigma_{ab}^2 g_{ab} (\sigma_{ab}) \times (\pi\gamma)^{1/2} (\gamma v)^{3/2} j_0(k\sigma_{ab}).$$

From (3.3) we can obtain  $\Lambda_{aa}^N$ ,  $\Lambda_{ab}^N$ , and  $\alpha_{aa}^N$ . The  $bb$  and  $ba$  matrix elements are obtained by changing  $a \rightleftharpoons b$  and  $\gamma \rightleftharpoons v$ . Three symmetry properties of the memory-function matrix elements should be noted: when  $n+n'$  is odd, the elements are real and vanish at small  $k\sigma_a$ ; when  $n+n'$  is even, the elements are purely imaginary and approach a constant in the small  $k\sigma$  limit, and  $M_{a\beta}^{cc}(i|j) = M_{\beta\alpha}^{cc}(j|i)$ .

### B. Memory function and mean-field term

The mean-field term in  $\phi_{\alpha\beta}$  is formed from two contributions. The first comes from the static part of  $\phi^s$  and has the form

$$M_{ab}^s = -n_a V_0^b \left[\frac{\gamma}{v}\right]^{1/2} k \Lambda_{ab} \delta_{0l} \delta_{0l'} \delta_{0m} \delta_{0m'} \delta_{1n} \delta_{0n'}, \quad (3.4)$$

with

$$\Lambda_{ab} = -4\pi\sigma_{ab} \frac{j_1(k\sigma_{ab})}{k}.$$

The second contribution is a part of the collision memory function. For example,

$$M_{ab}^{(cc)(m)} = -4\pi n_a g_{ab} \sigma_{ab}^2 V_0^b \left[\frac{\gamma}{v}\right]^{1/2} j_1(k\sigma_{ab}) \times \delta_{0l} \delta_{0l'} \delta_{0m} \delta_{0m'} \delta_{1n} \delta_{0n'}. \quad (3.5)$$

The sum of those two terms varies like  $g_{\alpha\beta} - 1$ . At very low density,  $g_{\alpha\beta}$  goes to unity and the mean-field terms go to zero. This is the term which describes the nonideality correction in the generalized Enskog equation.

## IV. NUMERICAL RESULTS

The parameter values which have to be specified for numerical computation, aside from densities, masses, and fluid temperature, are the hard-sphere diameters  $\sigma_\alpha$  and the pair distribution functions at contact. We will use the expression<sup>10</sup>

$$g_{\alpha\alpha}(\sigma^\alpha) = \left[1 + \frac{1}{2}\eta + \frac{3}{2}\eta_\beta \left[\frac{\sigma^\alpha}{\sigma^\beta} - 1\right]\right] (1-\eta)^{-2}, \quad (4.1)$$

$$g_{ab}(\sigma^{ab}) = \frac{1}{2\sigma^{ab}} (\sigma^b g_{aa} + \sigma^a g_{bb}),$$

$$\eta = \frac{\pi}{6} [n_a (\sigma^a)^3 + n_b (\sigma^b)^3] \equiv \eta_a + \eta_b, \quad (4.2)$$

where  $\eta$  is the packing fraction. The numerical solution of (2.4) has been programmed on a computer, and results have been obtained as dynamic structure factors defined

TABLE II.  $M_{aa}^{cc}(i|j)$  in units of  $n_b v_0^2 \sigma_{ab}^2 g_{ab} \sqrt{\pi\gamma}$ .

	$ 000\rangle$	$ 001\rangle$	$ E\rangle$	$ \sigma\rangle$	$ H\rangle$
$ 000\rangle$	0	0	0	0	0
$ 001\rangle$	0	$-i\frac{8}{3}$	0	0	$-i\frac{4\gamma}{3\sqrt{10}}$
$ E\rangle$	0	0	$-i\frac{8}{3}v$	0	0
$ \sigma\rangle$	0	0	0	$-i\frac{8}{15}(3\gamma+5v)$	0
$ H\rangle$	0	$-i\frac{4\gamma}{3\sqrt{10}}$	0	0	$-2i\left[\frac{v^2}{6} - \frac{11}{15}\gamma v - \frac{4}{5}\gamma + \frac{10}{3}\right]$

in (2.23). It is useful to characterize each spectrum by a dimensionless collision parameter<sup>2</sup> for each species

$$Y_\alpha = 0.41(P_\alpha/kv_\alpha\eta_\alpha), \quad (4.3)$$

where  $P_\alpha$  is the partial pressure,  $k$  the wave number,  $v_\alpha = (m_\alpha\beta)^{-1/2}$ , and  $\eta_\alpha$  the shear viscosity coefficient. Depending on the values of these parameters compared to unity, one can expect the spectrum to show hydrodynamic ( $Y > 1$ ) or kinetic ( $Y \lesssim 1$ ) behavior.<sup>7</sup>

The systems for which numerical results will be discussed are Xe-He mixtures at  $T=293$  K and various partial pressures. For a given mixture the dynamic structure factor  $S(\mathbf{k},\omega)$  is a linear combination of contributions from different species weighted by appropriate atomic polarizabilities [see Eq. (5.1)]. The various physical constants used are given in Table III. The  $k$  value in all the spectra presented in this work is  $k=1.727 \times 10^5 \text{ cm}^{-1}$  which is determined by the experimental condition of the light-scattering experiment.<sup>6</sup>

As a check of our calculations we consider first a pure fluid as a limiting case. Figure 1 shows a comparison of results for a case where the concentration of one of the two components is negligible with a kinetic model for a pure fluid,<sup>4</sup> the latter being known to give a good description of light-scattering spectra of moderately dense Xe gases. While thermal diffusion effects clearly can be ignored at this condition, the comparison does demonstrate that nonideality corrections to perfect-gas behavior are being treated correctly. The spectrum in this case shows characteristic hydrodynamic features of pronounced central and side peaks, as one may expect from the value of the collision parameter  $Y_{\text{Xe}}$ . The good agreement between the two kinetic models means that our formulation will behave properly in the hydrodynamic region of small  $k$ .

## V. APPLICATION TO LIGHT SCATTERING IN MODERATELY DENSE GAS MIXTURE

In light-scattering experiments the observed Rayleigh-Brillouin spectrum of a mixture is related to the various dynamical structure factors  $S_{\alpha\beta}(\mathbf{k},\omega)$  by the relation

$$S(\mathbf{k},\omega) \sim \alpha_a^2 n_a S_{aa}(\mathbf{k},\omega) + \alpha_b^2 n_b S_{bb}(\mathbf{k},\omega) + \alpha_a \alpha_b [n_a S_{ba}(\mathbf{k},\omega) + n_b S_{ab}(\mathbf{k},\omega)] \quad (5.1)$$

where  $\alpha$  is atomic polarizability. The experimental setup for the study of moderately dense mixtures has been described elsewhere.<sup>6</sup> The light source was a 171 Ar<sup>+</sup> Spectra Physics laser. The 5145-Å beam was monomode

TABLE III. Hard-sphere radii  $\sigma_i$ , polarizabilities  $\alpha_i$  (Ref. 6), and pair correlation at point of contact used in numerical calculations.

	$\sigma_{\text{Xe}}=4.79 \text{ \AA}$		$\sigma_{\text{He}}=2.17 \text{ \AA}$		
	$\alpha_{\text{Xe}}=3.999 \times 10^{24} \text{ cm}^3$		$\alpha_{\text{He}}=0.204 \times 10^{-24} \text{ cm}^3$		
$P_{\text{Xe}}$ (atm)	5.97	5.97	5.97	3.75	1.82
$P_{\text{He}}$ (atm)	9.17	4.79	3.80	3.51	2.65
$g_{\alpha\beta}$	1.147	1.144	1.143	1.136	1.135

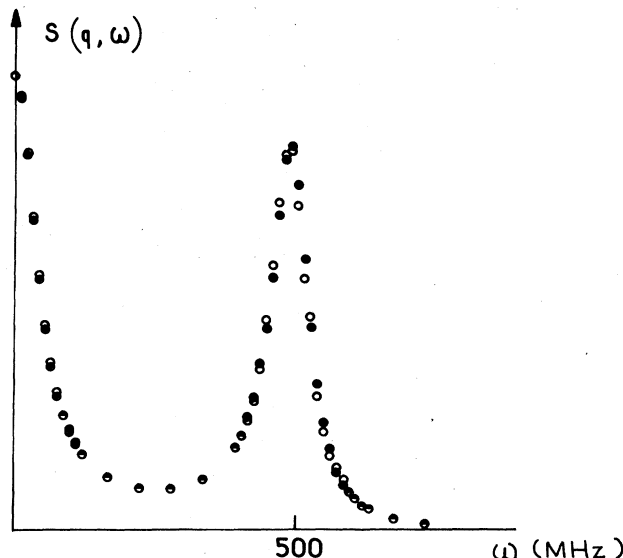


FIG. 1. Dynamic structure factor of gaseous Xe at  $P=5.97$  atm ( $Y_{\text{Xe}}=5.35$ ),  $T=293$  K, and  $k=1.727 \times 10^5 \text{ cm}^{-1}$ . Present calculation for  $P_{\text{He}}/P_{\text{Xe}} \sim 10^{-4}$  (open circles) and results from a kinetic model for a pure fluid (Ref. 4).

and stabilized in frequency in order to eliminate jitters created principally by the noise of the cooling water. The four-arm gas cell was free of stray light and no peak at the laser frequency was observed. We used high-grade gas prepared by Society Air Liquide. High-pressure handling equipment ensured a precision better than 1% in the measured pressure. Computation of molar composition was done with the virial equation of state of a Lennard-Jones mixture.

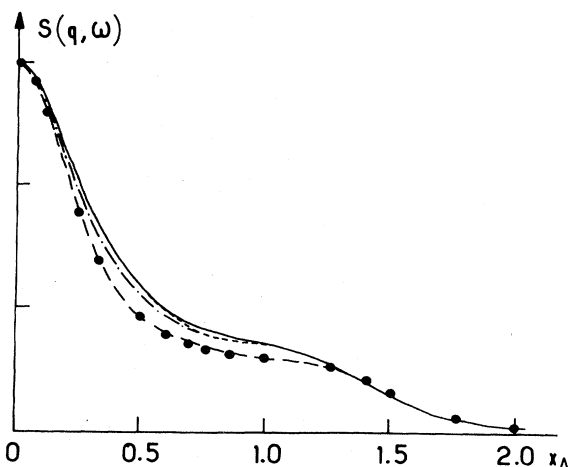


FIG. 2. Dynamic structure factor of Xe-He gas mixture at  $P_{\text{Xe}}=5.97$  atm ( $Y_{\text{Xe}}=5.35$ ),  $P_{\text{He}}=9.17$  atm ( $Y_{\text{He}}=1.667$ ). Frequency unit is  $X_A=530$  MHz. Symbols are as follows: —, full hydrodynamic calculation, Ref. 6; —, hydrodynamic calculation with  $K_T=0$  and no nonideality correction; - · - · -, hydrodynamic calculation with nonideality correction but  $K_T=0$ ; - - -, low-density kinetic model, Ref. 2; ●●●, present calculation.

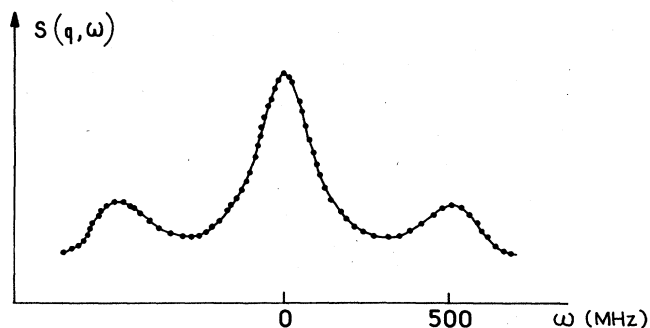


FIG. 3. Dynamic structure factor of Xe-He mixture at  $P_{\text{Xe}}=5.97$  atm ( $Y_{\text{Xe}}=5.35$ ),  $P_{\text{He}}=3.80$  atm ( $Y_{\text{He}}=0.69$ ). For this figure symbols are as follows: ●●●, experiment; —, present calculation.

Plane and spherical piezoelectrically scanned Fabry-Pérot étalon has a controlled finesse bigger than 45; photocounts were processed by a photon discriminator and sent to a multichannel analyzer. Instrumental profile was accurately fitted by an Airy function; it has been convolved with the theoretical spectra in the following comparisons with experimental data.

Figure 2 shows a comparison of the present kinetic model prediction with a hydrodynamic calculation which represents very closely the experimental spectra at this condition. The agreement indicates that our formulation describes the Xe-He system very well so far as density fluctuations at long wavelengths are concerned. One sees that imperfect-gas effects and thermal diffusions are both important, and these effects cause the central peak to become narrower. Notice also that the low-density kinetic model for Maxwell molecules is not able to give a satisfactory account of the data.

Nonhydrodynamic behavior in the Xe-He spectra are shown in Figs. 3–5. In going from Figs. 2 to 3 only the He concentration is decreased, and yet one observes a more pronounced propagating mode. This is an illustration of an enhanced damping of sound waves in a mixture which has been previously noted.<sup>5,11,6</sup> The experimental spectra in Figs. 3–5 cannot be well explained by the low-density kinetic model for Maxwell molecules. On the other hand, agreement with the present calculation is seen to be excellent. In Fig. 6 we show a comparison at lower Xe

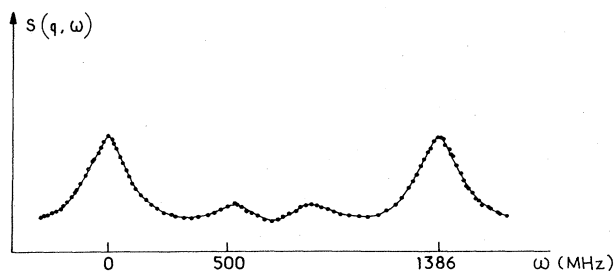


FIG. 4. Dynamic structure factor of Xe-He mixture  $P_{\text{Xe}}=5.97$  atm ( $Y_{\text{Xe}}=5.35$ ),  $P_{\text{He}}=4.79$  atm ( $Y_{\text{He}}=0.908$ ). For this figure symbols are as follows: ●●●, experiment; —, present calculation.

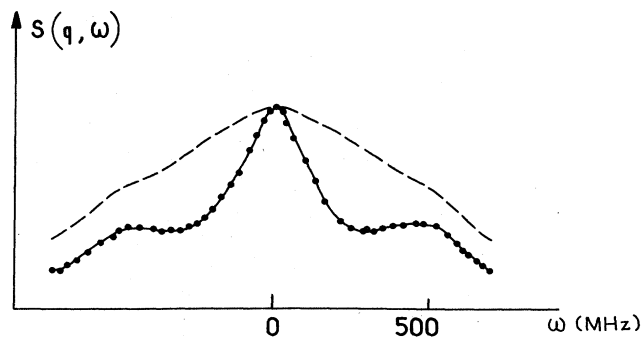


FIG. 5. Dynamic structure factor of Xe-He mixture at  $P_{\text{Xe}}=3.75$  atm ( $Y_{\text{Xe}}=3.36$ ),  $P_{\text{He}}=3.51$  atm ( $Y_{\text{He}}=0.64$ ). Symbols are as follows: ●●●, experiment; —, present calculation; — — —, hydrodynamic calculation.

and He pressures. Here, nonideality correction and thermal diffusion effects are much less important, and one has agreement between the kinetic models.

## VI. CONCLUDING REMARKS

We have developed a kinetic model for binary mixtures which is based on the generalized Enskog equations for hard spheres. This description is an improvement over an existing model<sup>2</sup> for dilute mixtures which was successful in explaining light-scattering spectra<sup>12</sup> of Xe-He systems at very low Xe pressure and small Xe molar fraction, conditions under which imperfect-gas effects and thermal diffusion can be ignored.<sup>6</sup> More recent data on Xe-He mixtures have shown that at higher pressures and larger molar fractions those effects are significant and that an extension of the kinetic model for Maxwell molecules is needed.<sup>7</sup>

The formulation of the present model follows closely a previous derivation<sup>5</sup> where it was already recognized that

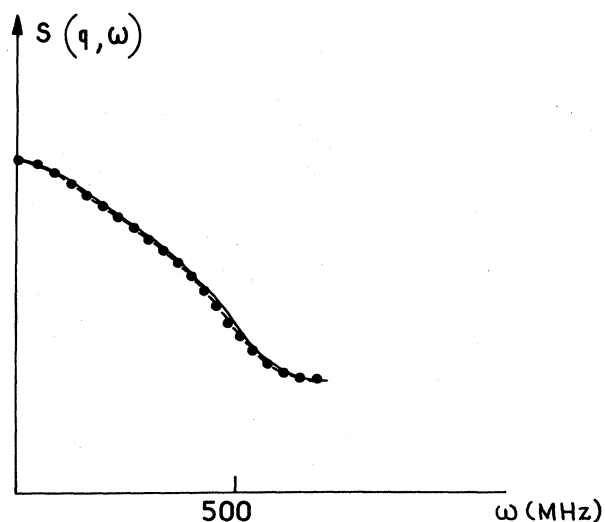


FIG. 6. Dynamic structure factor of Xe-He mixture at  $P_{\text{Xe}}=1.82$  atm ( $Y_{\text{Xe}}=1.63$ ),  $P_{\text{He}}=2.65$  atm ( $Y_{\text{He}}=0.48$ ). Symbols for this figure are the following: ●●●, experiment; —, low-density kinetic model (Ref. 2); — — —, present calculation.

the generalized Enskog equation provides an effective extension of the linearized Boltzmann equation to high densities.<sup>1</sup> The previous work was lacking in two respects, an important state representing the longitudinal part of the stress tensor was not included in constructing the kinetic model (see Sec. III), and numerical calculations were not carried out far enough to allow the model to be used for comparison with later experiments.<sup>6</sup> As we show in this work, a quantitative test of the Enskog theory can be made by comparing density-fluctuation spectra with light-scattering measurements. The theory is able to account for the effects of nonideality and thermal dif-

fusion,<sup>13</sup> and judging from the success of the Enskog theory for pure fluids,<sup>14</sup> our model should be useful over a wide range of densities.

#### ACKNOWLEDGMENTS

We are grateful to P. Maraval for help in numerical computation which was carried out on an IBM-3080D computer of C.N.U.S.C. (Montpellier). The work of one of us (S.Y.) was supported by the National Science Foundation. Centre de Physique Moléculaire Optique et Hertzienne is Laboratoire No. 238 associé au Centre National de la Recherche Scientifique.

#### APPENDIX

We will describe the evaluation of a typical matrix of the memory function. Starting from (2.14) we have

$$M_{ab}(i|j) = 2i \frac{n_a V_0^b}{\pi^3} (\sigma^{ab})^2 g_{ab} (\sigma^{ab}) v^{-2} \gamma^{-2} \int d^3\alpha d^3p d\Omega \exp \left[ - \left[ \frac{p^2}{\gamma} + \frac{\alpha^2}{v} \right] \right] (\mathbf{r} \cdot \mathbf{p}) \Theta(-\mathbf{r} \cdot \mathbf{p}) e^{i\mathbf{k} \cdot \hat{\mathbf{r}} \sigma^{ab}} \times \psi_j(\alpha/\varepsilon - \varepsilon \mathbf{p}) [\psi_i(\alpha - \mathbf{p}) - \psi_j(\alpha - \mathbf{p} + 2\mathbf{r}(\mathbf{r} \cdot \mathbf{p}))], \quad (\text{A1})$$

where  $\varepsilon = \sqrt{v}/\gamma$ ,  $\hat{\mathbf{r}}$  is unit vector in  $\mathbf{r}$  direction,  $\Omega$  is the solid angle. Post-collision momentum is of the form

$$\mathbf{p}^* = \mathbf{p} - 2\hat{\mathbf{r}}(\hat{\mathbf{r}} \cdot \mathbf{p}).$$

For the basis functions  $\psi_\alpha$  we use the standard Hermite polynomial. As an example we calculate the  $\langle \sigma | \psi_{ab}^{cc} | 001 \rangle$  term in Table I. From (3.1) we find

$$M_{ab}(\sigma | 001) = \left[ \frac{3}{2} \right]^{1/2} \left[ (M_{ab}(002 | 001) - \frac{1}{\sqrt{3}} M_{ab}(E | 001)) \right]. \quad (\text{A2})$$

It is sufficient to evaluate only the first term. The second term is composed of matrix elements of the same type,  $M_{ab}(002 | 001)$ ,  $M_{ab}(020 | 001)$ , and  $M_{ab}(200 | 001)$ .  $M_{ab}(i|j) = K_{ab} I_{M_{ab}}(i|j)$ , where  $K_{ab}$  is a constant and

$$I_{M_{ab}}(002 | 001) = \int d^3\alpha d^3p d^3r e^{i\mathbf{k} \cdot \mathbf{r}} \Theta(-\mathbf{r} \cdot \mathbf{p}) \psi_{001}(\alpha/\varepsilon + \varepsilon \mathbf{p}) [\psi_{002}(\alpha - \mathbf{p}) - \psi_{002}(\alpha - \mathbf{p} + 2\mathbf{r}(\mathbf{r} \cdot \mathbf{p}))]. \quad (\text{A3})$$

Introducing Hermite polynomials  $H_l(\xi_i)$  we have the basis function

$$\psi_{002}(\xi) = \frac{\xi_z^2 - 1}{\sqrt{2}}, \quad \psi_{001}(\xi) = \xi_z$$

with  $z$  along the  $k$  direction. Note that

$$\int e^{-\beta u^2} u^m du = \beta^{-(m+1)/2} \Gamma((m+1)/2) \quad (\text{A4})$$

if  $m$  is even and  $\Gamma(n)$  is the gamma function. Then

$$I_{M_{ab}}(002 | 001) = \frac{-4}{\sqrt{2}} \left[ \frac{I_1}{\varepsilon} - I_2 \varepsilon + I_3 \varepsilon \right], \quad (\text{A5})$$

where

$$\begin{aligned} I_1 &= \int d\Omega d^3\alpha d^3p e^{i\mathbf{k} \cdot \mathbf{r}} \Theta(-\mathbf{r} \cdot \mathbf{p}) e^{-(p^2/\gamma + \alpha^2/v)} (\mathbf{r} \cdot \mathbf{p})^2 \alpha_z^2 r_z, \\ I_2 &= \int d\Omega d^3\alpha d^3p e^{i\mathbf{k} \cdot \mathbf{r}} \Theta(-\mathbf{r} \cdot \mathbf{p}) e^{-(p^2/\gamma + \alpha^2/v)} (\mathbf{r} \cdot \mathbf{p})^2 p_z^2 r_z, \\ I_3 &= \int d\Omega d^3\alpha d^3p e^{i\mathbf{k} \cdot \mathbf{r}} \Theta(-\mathbf{r} \cdot \mathbf{p}) e^{-(p^2/\gamma + \alpha^2/v)} (\mathbf{r} \cdot \mathbf{p})^3 p_z^2 r_z. \end{aligned} \quad (\text{A6})$$

We give only the calculation of one of these integrals,

$$I_1 = \int d\Omega e^{i\mathbf{k} \cdot \mathbf{r}} r_z \int d^3p e^{-p^2/\gamma} (\mathbf{r} \cdot \mathbf{p})^2 \Theta(-\mathbf{r} \cdot \mathbf{p}) \int d^3\alpha e^{-\alpha^2/v} \alpha_z^2. \quad (\text{A7})$$

Using (A4) for  $m$  even, we have

$$\int d^3\alpha e^{-\alpha^2/v\alpha_z^2} = \frac{1}{2}\pi^{3/2}v^{5/2}. \quad (\text{A8})$$

To evaluate the  $p$  integral we consider first the identity

$$(\hat{\mathbf{r}} \cdot \mathbf{p})^n \Theta(-\mathbf{r} \cdot \mathbf{p}) = \lim_{\varepsilon \rightarrow 0} \left[ \int_{-\infty}^{+\infty} \frac{d\omega}{2\pi i} \frac{i^n}{\omega - i\varepsilon} \frac{\partial^n}{\partial \omega^n} e^{-i\omega \hat{\mathbf{r}} \cdot \mathbf{p}} \right]. \quad (\text{A9})$$

Then

$$I_1 = \frac{\pi^{3/2}v^{5/2}}{2} \int d\Omega e^{i\mathbf{k} \cdot \mathbf{r}_z} \int_{-\infty}^{+\infty} \frac{d\omega}{2\pi i} \frac{i^2}{(\omega - i\varepsilon)} \frac{\partial^2}{\partial \omega^2} \int d^3p e^{-p^2/\gamma - i\omega \mathbf{r} \cdot \mathbf{p}}. \quad (\text{A10})$$

The last integral is of the form

$$\int d^3p e^{-p^2/\gamma - i\omega \mathbf{r} \cdot \mathbf{p}} p_1^k p_2^l p_3^m = \pi^{3/2} \gamma^{(3+k+l+m)/2} (2i)^{-(k+l+m)} e^{-\gamma \omega^2/4} H_k(x_1) H_l(x_2) H_m(x_3), \quad (\text{A11})$$

where  $x_i = \sqrt{\gamma} \omega r_i/2$ . Now

$$I_1 = -\frac{\pi^3 v^{5/2} \gamma^{3/2}}{4\pi i} \int d\Omega e^{i\mathbf{k} \cdot \mathbf{r}_z} \int \frac{d\omega}{\omega - i\varepsilon} \frac{\partial^2}{\partial \omega^2} e^{-\gamma \omega^2/4}. \quad (\text{A12})$$

Using the Plemelj  $j$  identity

$$\lim_{\varepsilon \rightarrow 0} \frac{1}{\omega - i\varepsilon} = P \left[ \frac{1}{\omega} \right] + i\pi \delta(\omega)$$

we obtain

$$I_1 = \frac{\pi^3 v^{5/2} \gamma^2}{8} \int d\Omega e^{i\mathbf{k} \cdot \mathbf{r}_z}. \quad (\text{A13})$$

For integration over solid angle we use the integral relation

$$\int d\Omega r_1^k r_2^l r_3^m e^{i\mathbf{k} \cdot \hat{\mathbf{r}}_3 \sigma^{ab}} = \sigma^k \sigma^l \Gamma[(k+1)/2] \Gamma[(l+1)/2] (-i)^m 2^{(4+k+l)/2} \left[ \frac{\partial^m}{\partial X^m} \left[ \frac{J_{(k+l)/2}(X)}{X^{(k+l)/2}} \right] \right]_{X=k\sigma^{ab}}, \quad (\text{A14})$$

where  $\sigma^j = \frac{1}{2}[1 + (-1)^j]$  and  $j_\alpha(X)$  is the spherical Bessel function of order  $\alpha$ . Thus we find for  $I_1(X)$ ,

$$I_1 = -i \frac{\pi^4 v^{5/2} \gamma^2}{2} j_0'(X). \quad (\text{A15})$$

Using the same method we obtain for the other integrals in (A6)

$$I_2 = i\pi^4 v^{3/2} \gamma^3 \left[ j_0'''(X) - \frac{j_0'(X)}{2} \right], \quad (\text{A16})$$

$$I_3 = i\frac{3}{2}\pi^4 v^{3/2} \gamma^3 j_0'''(X).$$

Introducing  $I_1$ ,  $I_2$ , and  $I_3$  in (A5) gives

$$M_{ab}(002 | 001) = n_a v_0^b g_{ab}(\sigma^{ab})(\sigma^{ab})^2 \frac{4\pi}{\sqrt{2}} j_0'''(k\sigma^{ab}). \quad (\text{A17})$$

Using the relation

$$j_0'''(X) = \frac{1}{5}[3j_1(X) - 2j_3(X)],$$

and combining with the result for  $M_{ab}(E | 001)$  from Table I, we get finally

$$M_{ab}(\sigma | 001) = \frac{8\pi}{15} \frac{3/2}{15} n_a v_0^b g_{ab}(\sigma^{ab})(\sigma^{ab})^2 (j_1(X) - \frac{3}{2}j_3(X)). \quad (\text{A18})$$

This is the desired expression in Table I.

<sup>1</sup>For a review, see S. Yip, *Annu. Rev. Phys. Chem.* **30**, 547 (1979).

<sup>2</sup>C. D. Boley and S. Yip, *Phys. Fluids* **15**, 1424 (1972).

<sup>3</sup>P. Furtado, G. Mazenko, and S. Yip, *Phys. Rev. A* **13**, 1641

(1976).

<sup>4</sup>L. Letamendia, E. Leutheusser, and S. Yip, *Phys. Rev. A* **25**, 1222 (1982).

<sup>5</sup>J. I. Castresana, G. F. Mazenko, and S. Yip, *Ann. Phys. (N.Y.)*

- 103, 1 (1977); Phys. Rev. A 14, 1814 (1976).
- <sup>6</sup>L. Letamendia, Ph.D. thesis, University of Bordeaux, 1979; L. Letamendia, J. P. Chabrat, G. Nouchi, J. Rouch, C. Vaucamps, and S. H. Chen, Phys. Rev. A 24, 1574 (1981).
- <sup>7</sup>L. Letamendia, P. Joubert, J. P. Chabrat, J. Rouch, C. Vaucamps, C. D. Boley, S. Yip, and S. H. Chen, Phys. Rev. A 25, 481 (1982).
- <sup>8</sup>E. P. Gross and E. A. Jackson, Phys. Fluids 2, 432 (1959).
- <sup>9</sup>*Handbook of Mathematical Functions*, edited by M. Abramowitz and I. Stegun (Dover, New York, 1965).
- <sup>10</sup>J. L. Lebowitz, Phys. Rev. 133 A, 896 (1964).
- <sup>11</sup>W. S. Gornall and C. S. Wang, J. Phys. (Paris) 33, C1-51 (1972).
- <sup>12</sup>N. A. Clark, Phys. Rev. A 12, 2092 (1975).
- <sup>13</sup>For a discussion of the application of Enskog theory to the calculation of transport coefficients in mixtures, see M. Lopez de Haro, E. G. D. Cohen, and J. M. Kincaid, J. Chem. Phys. 78, 2746 (1983).
- <sup>14</sup>W. E. Alley, B. J. Alder, and S. Yip, Phys. Rev. A 27, 3174 (1983).